JOURNAL OF GEOPHYSICAL RESEARCH, VOL. 106, NO. A4, PAGES 6043–6057, APRIL 1, 2001

Electrostatic electron cyclotron waves observed by the plasma wave instrument on board Polar

J. D. Menietti, J. S. Pickett, D. A. Gurnett, and J. D. Scudder

Department of Physics and Astronomy, University of Iowa, Iowa City

Abstract. We report the results of an investigation of waves observed by the Polar spacecraft at high altitudes and latitudes and at frequencies just above the cyclotron frequency. These observations are made frequently when the spacecraft is over the polar cap as well as near the dayside cusp and near the nightside auroral region, and observations are made for ratios of plasma frequency to cyclotron frequency, $f_p/f_c \sim 1$. Using the six-channel high-frequency waveform receiver (HFWR) on board the spacecraft, which can provide three-axis electric and three-axis magnetic field measurements, we attempt to identify the wavemode of these emissions and investigate possible source mechanisms including low-energy electron beams. We further observe electromagnetic emission associated with upper hybrid waves near and within the plasmasphere. This emission is consistent with both Z and O modes.

1. Introduction

Electrostatic electron cyclotron (EEC) waves have been studied for many years [cf. *Shaw and Gurnett*, 1975; *Kurth et al.*, 1979a, 1979b]. The observations have typically been obtained during crossings of the plasma sheet near the magnetic equator, where the ratio of plasma frequency f_p to cyclotron frequency f_c is typically much larger than 1 and where electron pitch angles are large. Intense noise bands are frequently observed in the plasmasphere at frequencies between f_p and the upper hybrid frequency $f_{UH} = \sqrt{(f_p^2 + f_c^2)}$ [*Mosier et al.*, 1973]. Original numerical studies have shown that the highest growth rates occur for $f_p/f_c > 1$ [cf. *Tataronis and Crawford*, 1970]. Bernstein mode waves [*Bernstein*, 1958] can grow, however, for both large and small ratios of f_p/f_c (cf. *Krall and Trivelpiece*, 1973], and the ratio f_p/f_c determines the precise location of the emission fundamental and harmonic frequencies. *Young et al.* [1973] have shown that a dense, warm electron distribution of electrons in the range $df/dv_\perp > 0$ can excite waves with $f_c < f < 1.5 f_c$ and that for $k_\parallel \neq 0$ a temperature anisotropy $T_\perp > T_\parallel$ can excite waves between f_c and 2 f_c. More recent investigations of electron cyclotron waves generated by beams and temperature anisotropies have been conducted for $f > f_c$ [*Winglee et al.*, 1992] and for $f < f_c$ [*Wong and Goldstein*, 1994].

Gurnett et al. [1983] have reported "3/2 f_c" emission in the cusp in the DE 1 plasma wave data at a radial distance of ~ 3.5 R_E, at a time when $f_p/f_c \leq 1$. *Farrell et al.* [1990] subsequently studied a number of examples of wave intensifications near f_c. They found that the waves most often occurred at times of large magnetic index *Kp*. For specific cases these authors found the waves to be oblique with wave normal angles varying from ~ 10° to ~ 60°. The electric field intensity of these waves was typically of the order of a few to tens of $\mu V\ m^{-1}$. This is much smaller than the large amplitude $(n+1/2)\ f_c$ oscillations observed by *Kurth et al.* [1979a, 1979b] inside the plasmasphere.

Paper number 2000JA003016.
0148-0227/01/2000JA003016$09.00

The apogee of the Polar spacecraft over the northern polar cap during 1996 and 1997 was approximately 9 R_E, and the spacecraft often entered a region where $f_p \geq f_c$, because the cyclotron frequency falls off more rapidly with radial distance than the plasma frequency. In this paper we present observations of intense EEC waves and harmonics, which have not been typically observed at high latitudes and altitudes of the polar magnetosphere but which are frequently observed by the plasma wave instrument on board Polar. DE 1 did sample the midaltitude polar regions but typically at radial distances of 3-4 R_E compared with 7-9 R_E for Polar. We mention that EEC waves similar to those discussed in this paper are also observed by Polar in the turbulent boundary layer of the cusp [cf. *Pickett et al.*, this issue]. Upper hybrid waves observed by Polar near and within the plasmasphere are seen to be associated with electromagnetic emission that has a magnetic component that is consistent with O and Z modes. These observations probably have a free energy source of electron beams and anisotropic electron distributions.

2. Instrumentation

The Polar satellite was launched in late February 1996 into a polar orbit with an apogee of ~ 9 R_E and a perigee of ~ 2.2 R_E. Polar is the first satellite to have three orthogonal electric antennas (E_u, E_v, and E_z), three triaxial magnetic search coils, and a magnetic loop antenna, as well as an advanced plasma wave instrument [*Gurnett et al.*, 1995]. This combination can potentially provide the polarization and direction of the arrival of a signal without any prior assumptions.

The plasma wave instrument (PWI) on the Polar spacecraft is designed to provide measurements of plasma waves in the Earth's polar regions over the frequency range from 0.1 Hz to 800 kHz. Five receiver systems are used to process the data: a wideband receiver (WBR), a high-frequency waveform receiver (HFWR), a low-frequency waveform receiver, two multichannel analyzers, and a pair of sweep frequency receivers. For the high-frequency emissions of interest here the HFWR and WBR are of special importance. The WBR provides high-resolution waveform data and is programmable allowing the selection of 11, 22, or 90 kHz bandwidths with a lower band edge (base frequency) at 0, 125, 250, and 500 kHz. With the 11 kHz filter, the WBR sampling rate is

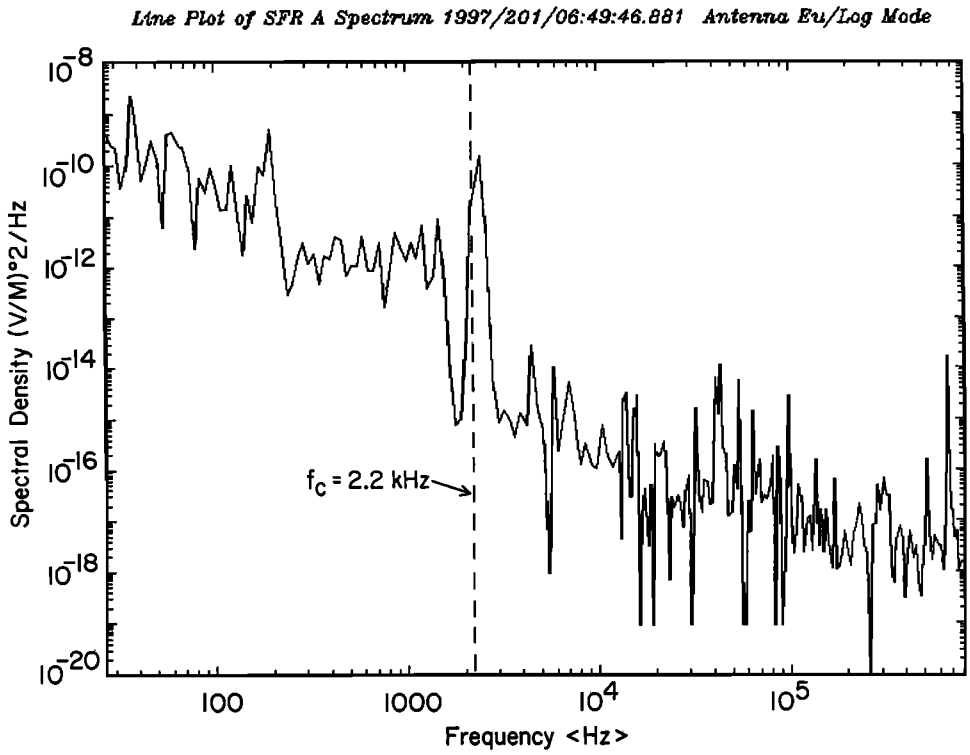

Figure 1. Power spectral density versus frequency for an ~ 32-s period beginning at 0649:46.881 UT. The dashed line indicates the electron cyclotron frequency. The spectral density of the electrostatic electron cyclotron (EEC) wave near f_c corresponds to an electric field intensity of ~ 0.097 mV m^{-1}.

31.12 kHz. The HFWR measures high-resolution waveform data using three orthogonal electric field antennas and three triaxial magnetic search coils. With the 25-kHz filter the sampling rate is 71.43 kHz.

The electron and ion hot plasma instrument (HYDRA) [*Scudder et al.*, 1995] is an experimental three-dimensional hot plasma instrument for the Polar spacecraft. It consists of a suite of particle analyzers that sample the velocity space of electron and ions between ~ 2 and 35 keV/q in three dimensions, with a routine time resolution of 1.5 s. The satellite has been designed specifically to study accelerated plasmas such as those in the cusp and auroral regions.

3. Observations

In Plate 1 we show a frequency-versus-time spectrogram of the swept frequency receiver (SFR) electric field (E_u) data for an 8.5-hour period on day 201 of 1997, when the Polar spacecraft was high over the polar cap and proceeded into the midafternoon auroral region. The frequency range is 100 Hz to 20 kHz. Clearly seen is whistler mode emission at frequencies $f < f_c$, where f_c is displayed by the white line. Also clearly seen are intense, highly electrostatic emissions in a relatively narrow band at frequencies just above f_c. Less intense, broadbanded electrostatic emission is often seen to extend well above f_c. These bursts are largely electrostatic emissions probably associated with beam-driven modes. In Plate 2 we display a two-panel plot of emissions for a 2.5-hour period from 0230 to 0430 UT. The top panel is the electric field intensity (E_u antenna), and the bottom panel is the magnetic field intensity (loop antenna). Plate 2 shows that the emission above f_c is essentially electrostatic or very weakly magnetic. Above ~ 300 Hz, however, the magnetic loop antenna is too insensitive to measure the signal due to whistler mode for typical values of wave intensity. In Plate 3 we display a high-resolution 48-s snapshot of the WBR for a frequency range of 0 to 10 kHz (Nyquist frequency of 10 kHz). The starting time of the plot is 0345:21.056 UT. Here the EEC waves are seen as harmonics of f_c. Since the harmonics lie close to integer multiples of f_c, this would indicate that $f_p/f_c \leq 1$ [cf. *Krall and Trivelpiece*, 1973].

In Plate 4 we show a spectrogram of the SFR electric and magnetic field intensity for the 30-min time interval from 0630 to 0700 UT. The bursty nature of the EEC waves and their frequent high intensity are obvious. The relatively intense bursts that extend in frequency beyond f_c are electrostatic, as confirmed by the magnetic field shown in the bottom panel. However, the magnetic loop receiver system is not very sensitive to the low-intensity whistler mode emission at frequencies in the range ~ 300 Hz $< f <$ f_c. Figure 1 shows the power spectral density versus frequency for an ~ 32-s time interval starting at 0649:47 UT. The dashed line indicates the value of $f_c = 2.2$ kHz. The large peak near this line is due to the EEC wave and indicates an electric field intensity of ~ 0.097 mV m^{-1}. The emission at $f < f_c$ is dominantly whistler mode and appears to have a cutoff just below f_c (top panel). However, this is misleading. In fact, we believe that at this time, $f_p \geq f_c$ and under these plasma conditions the whistler mode is cutoff at f_c instead of f_p. The spectrograms generally show a variable gap between the highest-frequency whistler mode emission and f_c. This gap is due to attenuation of the whistler mode as the frequency approaches f_c. There are periods of time such as between 0645 and 0648 UT when the gap appears to widen, but the whistler mode emission for $f < f_c$ is still present at a lower intensity level (green color) up to nearly f_c. In Figure 1 the whistler mode signal begins to fall off steadily, owing to attenuation at a frequency of 1.6 kHz reaching a minimum at 1.79 kHz, where the wave intensity begins to increase, owing to the bandwidth of the EEC emission which peaks at 2.45 kHz. The exact location of the whistler mode cutoff depends on the channel center frequency and the response function of the receiver channel. The data are consistent with a plasma frequency $f_p > f_c$. The density measurements of the hot plasma instrument (HYDRA) on board

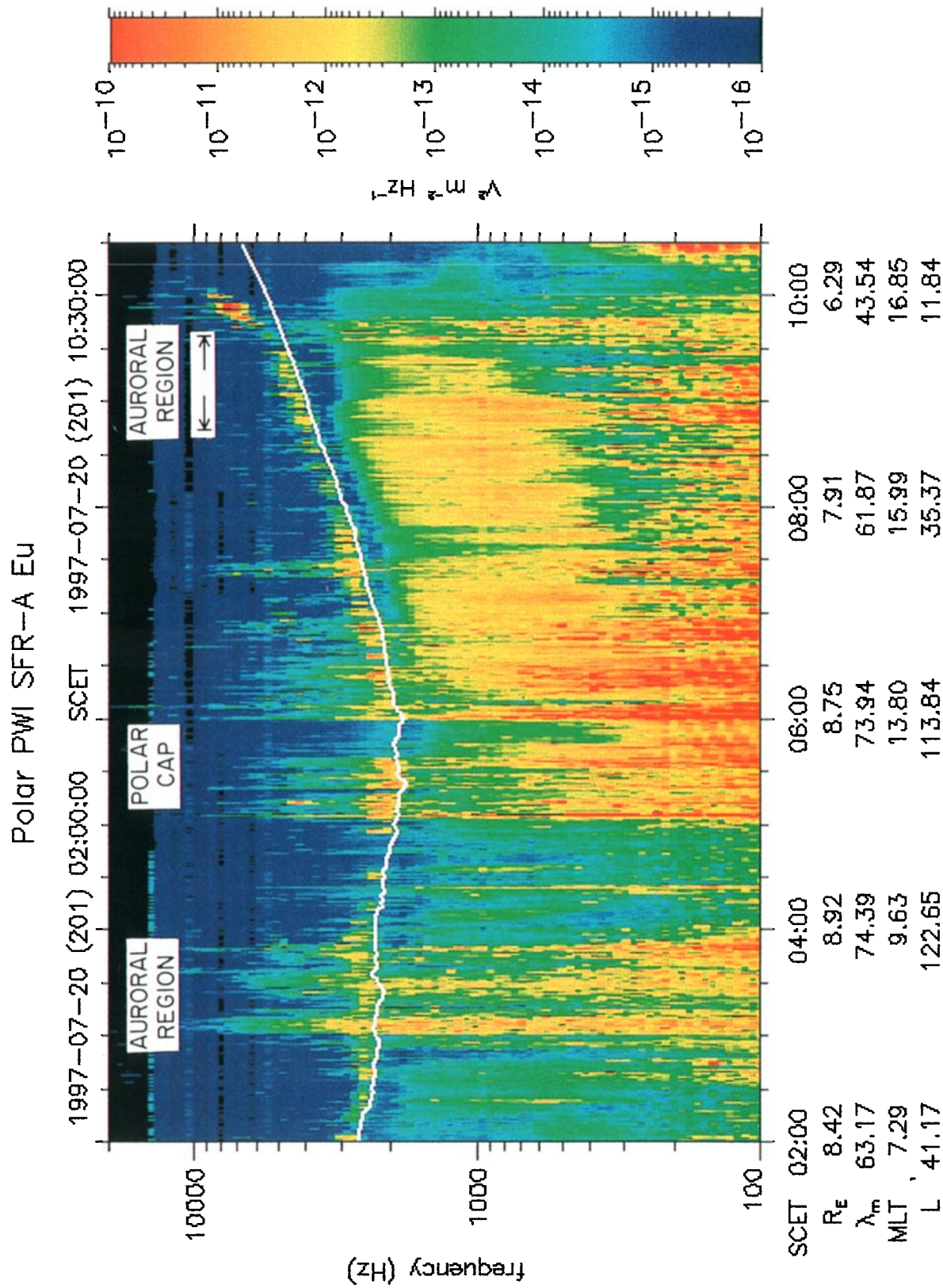

Plate 1. Frequency-versus-time spectrogram showing the electric field oscillations and the emissions in question as an often intense (yellow), relatively narrow band feature just above the cyclotron frequency (the white line). This survey plot covers 8.5 hours of July 20, 1997 (day 201). PWI, plasma wave instrument; SFR, swept frequency receiver.

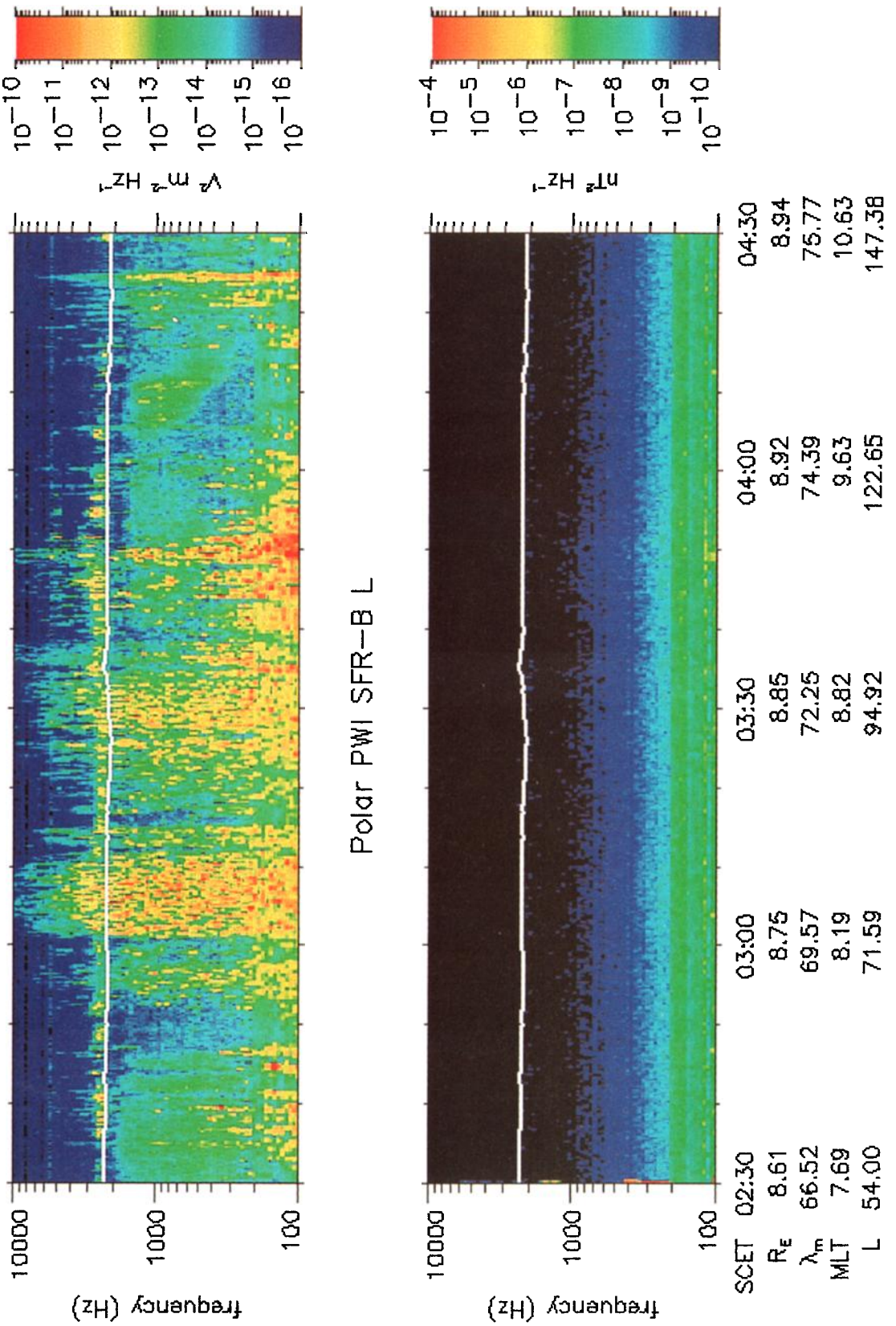

Plate 2. Frequency-versus-time spectrogram of the spectral densities for the (top) electric field and (bottom) magnetic field, showing the narrowbanded electrostatic emissions above the cyclotron frequency with frequent broadbanded bursts that extend from well below to well above f_c.

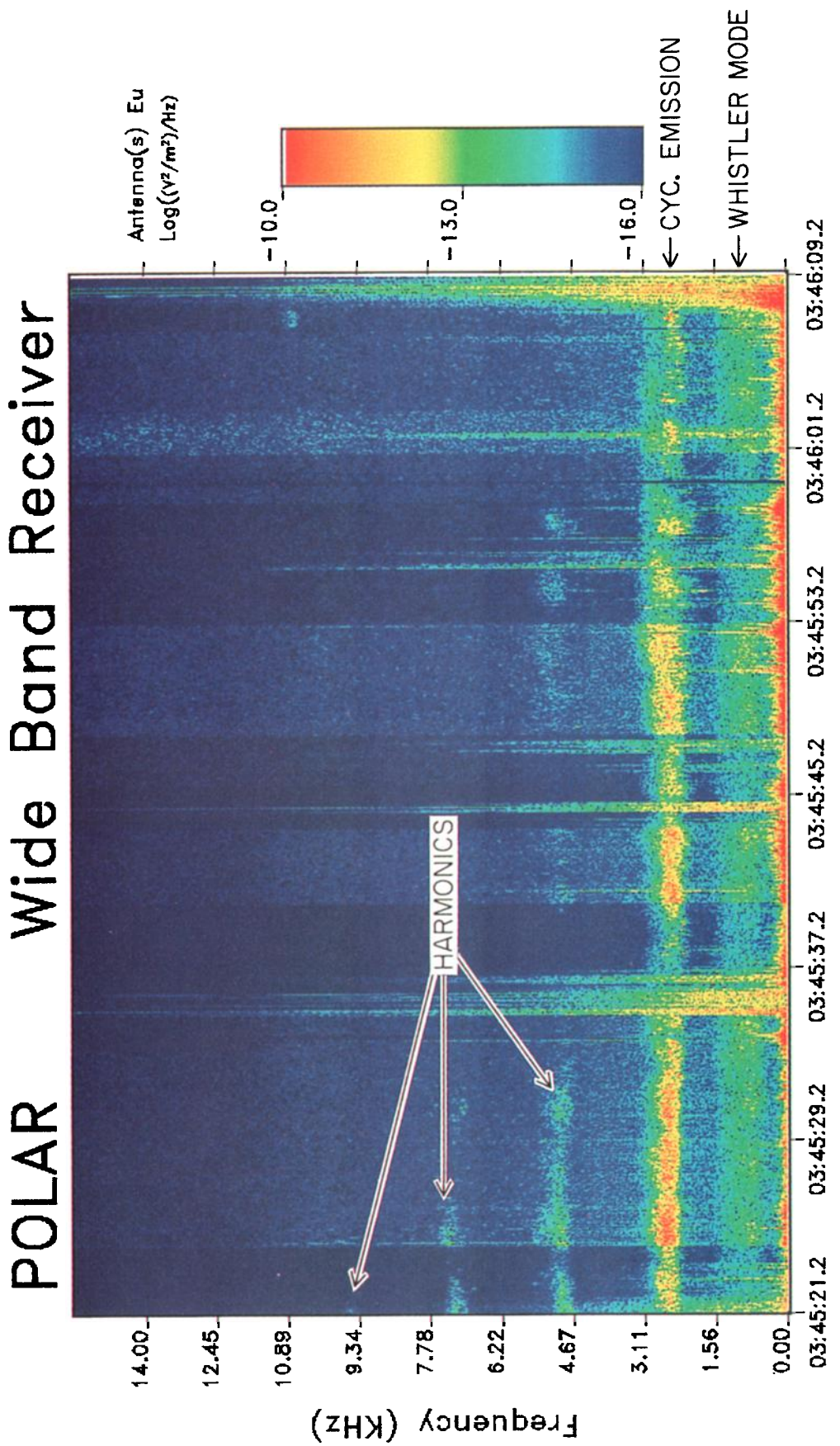

Plate 3. Wideband (high resolution) spectrogram of the electric field intensity for a 48-s time interval starting at 0345:21 UT of day 201. Note the fundamental and harmonics of the cyclotron emission at f_c and $n = 2$, 3, and 4.

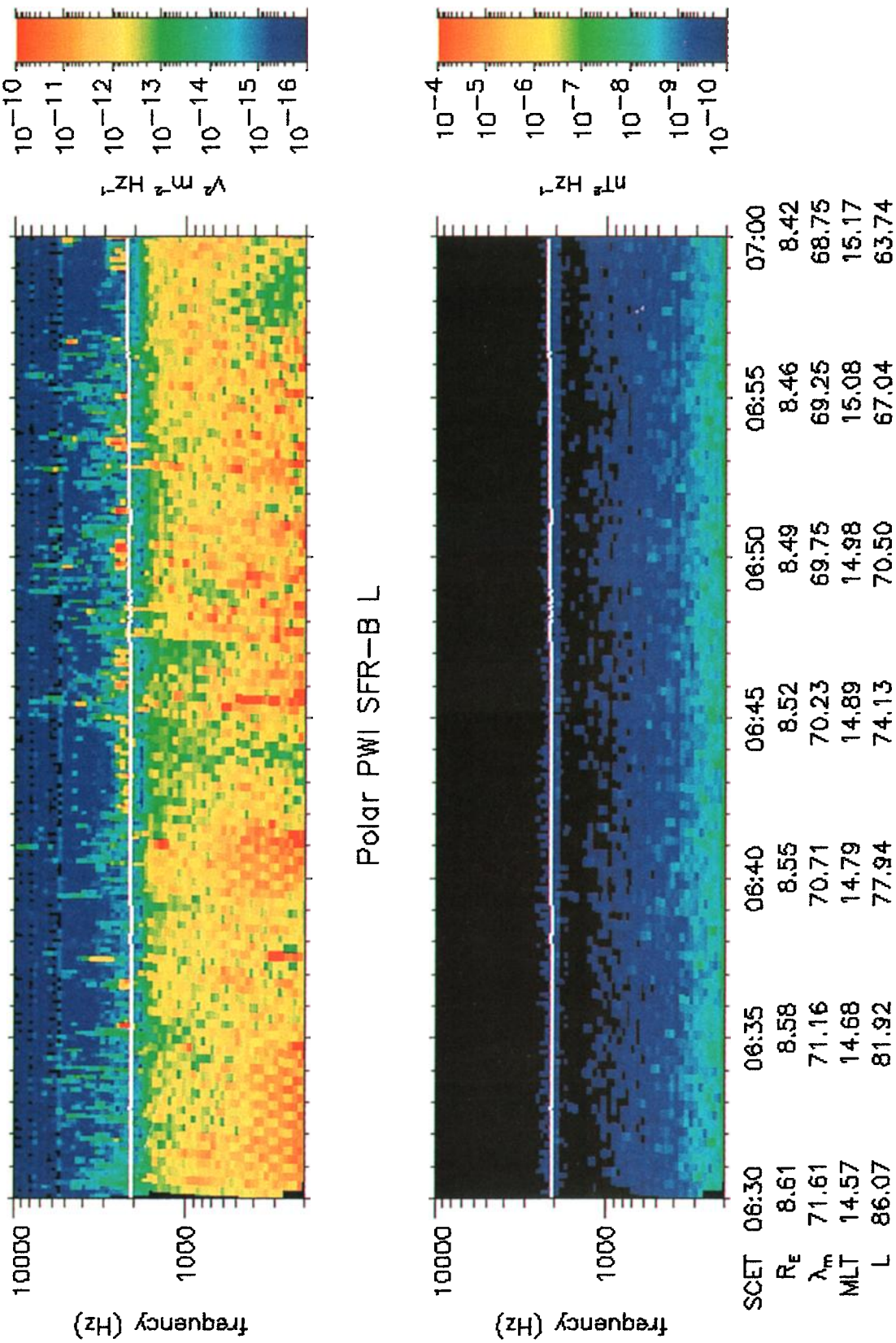

Plate 4. Spectrogram showing more narrowbanded emission above f_c. We believe the emission at $f < f_c$ is whistler mode, but the cutoff below f_c is probably an attenuation due to f_c rather than the plasma frequency f_p.

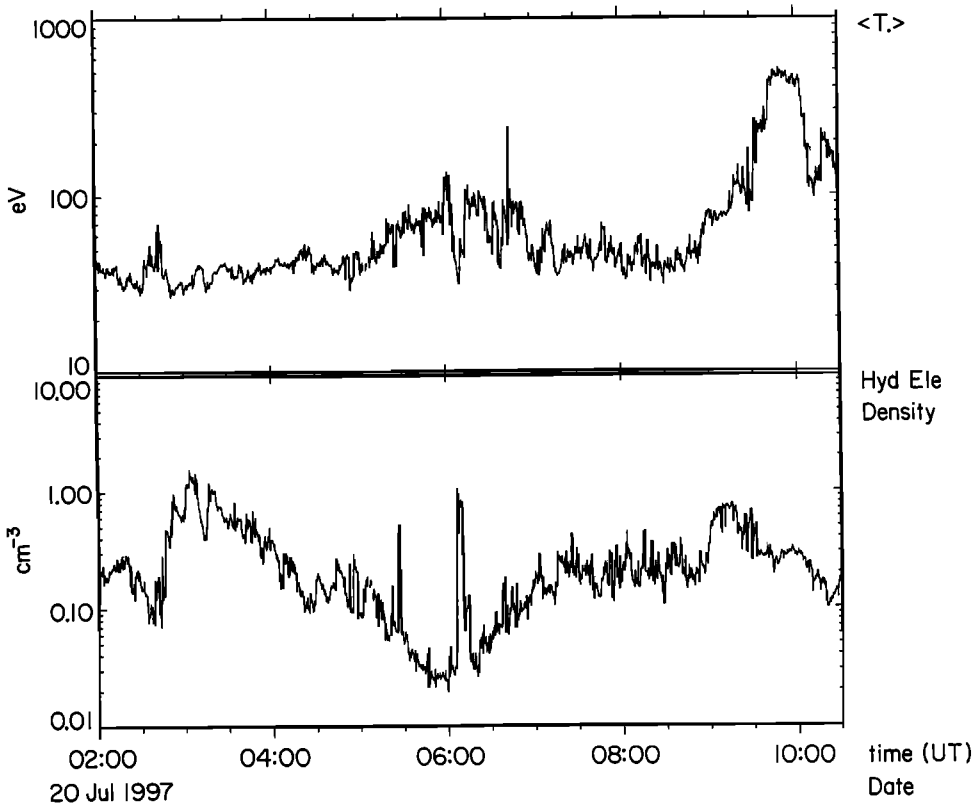

Figure 2. (top) Electron temperature and (bottom) number density (from HYDRA), for the times shown. The densities shown often indicate higher densities than those "indicated" by the whistler mode cutoff of the plasma wave instrument (PWI).

Polar support these high-density values. In Figure 2 we plot the electron temperature (top panel) and density calculations from HYDRA for the time interval 0200-1030 UT. Between 0630 and 0700 UT, for instance, the density is seen to rise rapidly from 0.05 to 0.10 cm^{-3}. Thus, $f_p > 2.0$ kHz, and f_p is higher than f_c for the entire interval. Because of the lower energy cutoff of the HYDRA instrument in the absence of spacecraft charging (~ 12 eV), it may be assumed that the HYDRA instrument would provide a lower limit to the plasma density. For times greater than ~ 0945 UT, the densities calculated from HYDRA are too low because of the presence of an undetected cold plasma population in and near the plasmasphere that is not accounted for.

The polarization of the emissions can be examined by plotting the time-tagged electric field components in field-aligned coordinates. Figure 3a is an example of such plots in the frequency rate 2 kHz $< f <$ 7 kHz for a time near 0650:13 UT. The left panel is a plot of the electric field in the plane perpendicular to the magnetic field for a total of 4.2 ms. Clearly, the electric field is largely perpendicular to B and shows, at this time, a left-handed polarization (LHP) sense. However, examining consecutive plots, we find no consistent sense of polarization, rather there are about as many cases of LHP as there are of right-handed polarization (RHP). Such an example is seen in Figure 3b starting only ~ 7 ms later. This is consistent with a linear polarization expected for electrostatic emission. The waves are measured independently from the three orthogonal antenna/receiver systems E_u, E_v, and E_z. A linearly polarized wave will thus show a random phase difference between receivers for E_u and E_v, for instance. Thus, in transforming the signals to a field-aligned coordinate system it is expected that the polarization will show a random "circular" polarization as we observe, with no preferred handedness.

Winglee et al. [1992] have shown that right-handed circular polarized electromagnetic emission can be generated by electron distributions with beams and temperature anisotropies ($T_\perp/T_\parallel > 1$) at frequencies above f_c for $0.67 < f_p/f_c \leq 1.0$. For $f_p/f_c \geq 1$ they found that most of the wave energy is left-hand circular polarized and is trapped (probably Z mode). However, the electron data indicate that the dominant distributions have $T_\parallel / T_\perp > 1$. In Plate 5a we plot the electron anisotropy (top panel) and skew from HYDRA for the period $0330 < t < 0400$, which spans the time of Plate 3 depicting electrostatic electron cyclotron harmonics. Plate 5b is a similar plot for the period 0640-0700 UT, during which EEC waves are seen in Plate 4. Plates 5a and 5b are corrected for spacecraft potential. Skew is defined as the difference between magnetic field-aligned and field-opposed fluxes at fixed energy. Yellow and red indicate net flux in the B field-aligned direction, and cyan and blue indicate net flux in the opposed direction. Black indicates that there is no experimentally significant difference between the measurements. Grey indicates that a useful calculation could not be performed. Skew is made dimensionless by dividing by the expected Poisson and other errors in the fluxes compared. Anisotropy indicates the difference between field-aligned and perpendicular spectra. Field-aligned and field-opposed spectra are averaged (with equal weights) and compared to the perpendicular spectrum, again in units of the expected error. The electrons near 0350 UT show a relatively strong field-opposed distribution for electrons at energies less than 1 keV. Plate 5b also indicates flows of electrons parallel to B at energies less than 1 keV, and the bottom panel shows that the beams are typically away from the Earth, especially near 0650 UT coincident with the EEC wave intensification near the same time. Near 0651 UT, red indicates a lower-energy electron beam traveling toward the Earth. To better illustrate these beams, we include

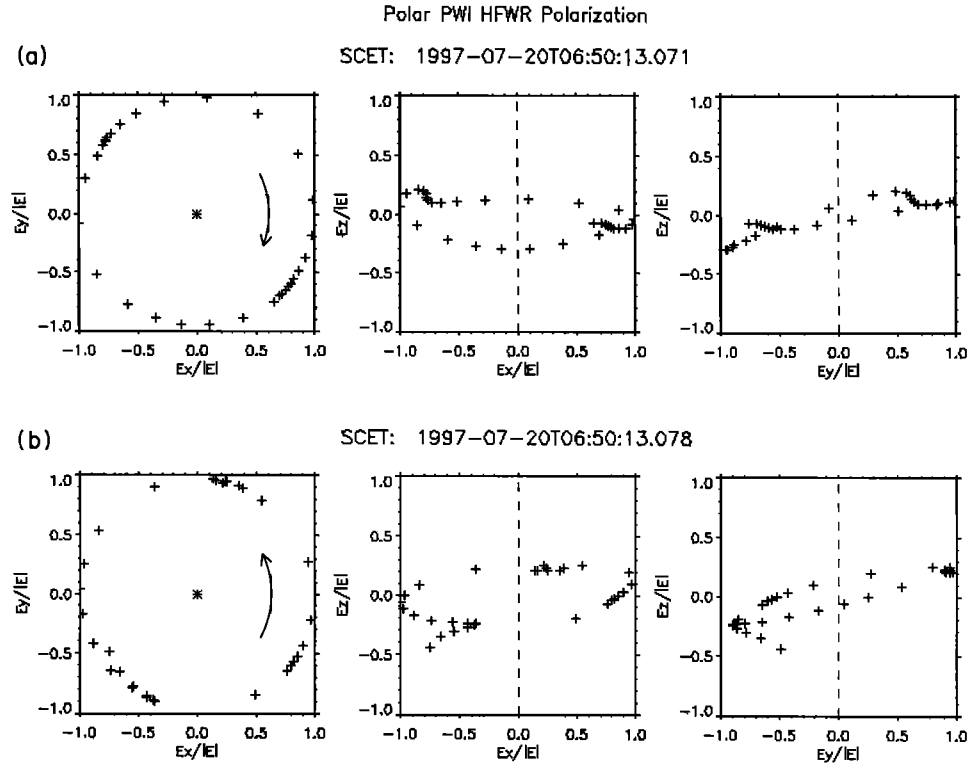

Figure 3. (a) Snapshot of the polarization of the electric field vector in magnetic field-aligned coordinates over the frequency range 2-7 kHz. The magnetic field direction is shown as an asterisk (field out of the page) in the left panel and as a dashed line in the middle and right panels. For this snapshot the wave appears to show left-hand circular polarization. (b) Snapshot for which the polarization appears to show right-hand polarization.

Figure 4a, which is a plot of contours of the electron distribution function in field-aligned velocity space for a two-spin period of time centered near 0350:04 UT. Clearly seen is an electron beam at $E <$ 1 keV moving up the field line (away from Earth). In Figures 4b and 4c we show similar plots for the period of time centered near 0649:28 and 0650:09 UT, respectively. Again, we see an electron beam moving up the field line in Figure 4b, while Figure 4c shows a warmer, less distinct beam moving down the field line. These beams are a likely source of free energy for the EEC waves.

In Plate 6 we show a spectrogram of emission for a time (0930-1100 UT) when the satellite approaches the plasmasphere and upper hybrid resonance (UHR) emission is present. The sensitivity of the loop antenna falls off rapidly above ~ 5 kHz, so the corresponding magnetic field spectrogram is omitted here but the magnetic field is shown using the HFWR in Figure 5. These narrowbanded signatures, which extend well above f_c, are typically observed near the plasmaspheric boundary and can be used to obtain the plasma density by $f_{UH}=\sqrt{(f_p^2+f_c^2)}$. The plasma frequency reaches a peak near 1030 UT inside the plasmasphere when f_{UH} ~ 27 kHz, f_p ~ 26 kHz, and n ~ 8.4 cm^{-3}. The whistler mode plasmaspheric hiss upper cutoff is typically well below the local plasma frequency inside the plasmasphere. Figure 5 shows the power spectral density versus frequency for an ~ 32-s time interval starting at 0953:53 UT. The dashed line indicates the value of f_c = 5.37 kHz. The large peak near this line is due to the EEC wave and indicates an electric field intensity of ~ 0.112 mV m^{-1}.

In Figure 6 we plot the measured index of refraction, cB/E, the magnitude of the electric field, and the magnetic field versus time for a period of time including some of the most intense emissions seen in Plate 6. Here we have assumed that $\bar{k} \perp \bar{E}$, an approximation that produces a minimum value of n. The measured electric fields at this time indicate that $E_\parallel/E_\perp \lesssim 0.10$. The time interval starts at 0954:03.867 UT and extends for 7.168 ms. This snapshot is typical of most for the intense emissions. The dominant high frequency of the waveform is nearly 7.65 kHz. The electric field has a slower modulation at a frequency of a few hundred hertz. The magnetic field is more bursty but has the same dominant high frequency, but an independent and irregular modulation at an approximate frequency of 2.0 kHz. These electromagnetic oscillations have indices of refraction that typically vary in the range $0 < n < 3$ and are consistent with Z mode ($f < f_{UH}$); $n > 1$) and O mode ($f > f_p$; $n < 1$).

In Figure 7 we plot the cold plasma index of refraction for a plasma with f_p = 5.0 kHz and f_c = 5.37 kHz similar to the parameters of the plasma believed to exist near 0954 UT. Figure 7a is for a wave normal angle of 10°, and Figure 7b is for a wave normal angle of 60°. Since the X mode does not propagate for frequencies less than f_{RX} ~ 8.4 kHz, the only possible modes are the O mode and Z mode, which show values of index of refraction n that are < 1 and > 1, respectively. The Z mode emission has a high-frequency cutoff near f_{UH} for large wave normal angle. This cutoff decreases in frequency for smaller wave normal angles. O mode emission can propagate at all wave normal angles for $f > f_p$. The electromagnetic emissions of Plate 6 are consistent with the O and Z modes.

4. Summary and Discussion

We have presented observations of intense narrowbanded emissions observed high above the polar cap at frequencies near and above the local cyclotron frequency. These emissions are consistent with electron cyclotron waves and harmonics (compare Plate 3). The electric fields are often nearly perpendicular to the ambient B. There are weak, if any, oscillations of the magnetic field present.

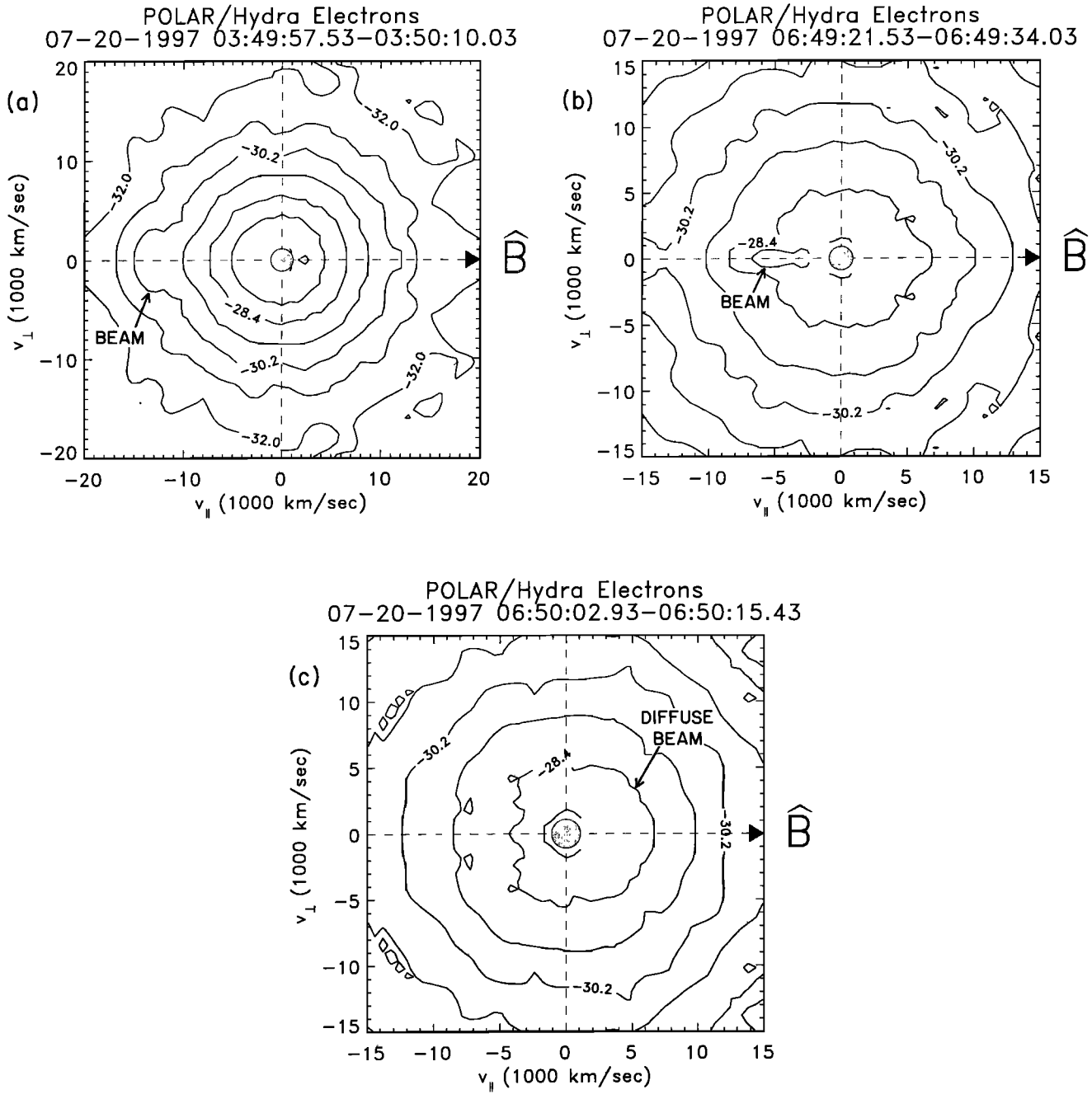

Figure 4. (a-c) Contours of the electron distribution function in velocity space for the time periods indicated. Each distribution is collected for a two-spin period of the satellite. In Figure 4a an electron beam with $E < 1$ keV is seen traveling up the field line away from Earth. In Figure 4b a similar electron beam but with somewhat lower energy and narrower pitch angle is seen traveling away from Earth. In Figure 4c, the adjacent time period shows a more diffuse electron beam traveling toward the Earth.

These waves are typically observed near the magnetic equator, where $f_p/f_c >> 1$, but have been reported in a relatively few cases of DE 1 data from the cusp and nightside auroral region, where $f_p/f_c \leq 1$ [*Gurnett et al.*, 1983; *Farrell et al.*, 1990]. Polar samples the same regions as DE 1 at considerably higher altitudes, where f_p/f_c can be greater than 1. We have presented a typical example of perhaps several hundred such cases observed by Polar when apogee was over the north polar cap. During July and August 1997, for example, every Northern Hemisphere pass showed EEC waves similar to those reported here. Our observations indicate that enhancements of emission near and above f_c are a common occurrence in the Polar plasma wave data. We observe whistler mode emission that often extends up to f_c, thus being consistent with HYDRA measurements of the density at values near and above f_c. The polarization measurements obtained near 0650:13 UT show both a left-handed sense and a right-handed sense.

Near the end of the time interval examined ($t > 0940$ UT) and near the plasmasphere boundary, PWI observes what appear to be

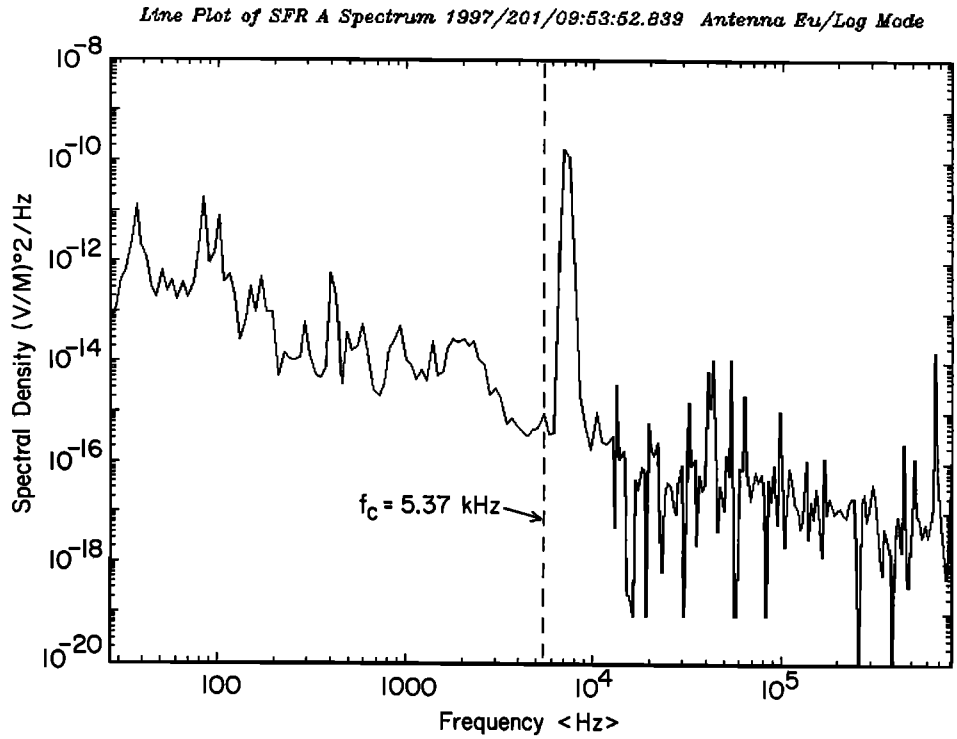

Figure 5. Power spectral density versus frequency for an ~ 32-s period beginning at 0953:52.839 UT. The dashed line indicates the electron cyclotron frequency. The spectral density of the EEC wave near f_c corresponds to an electric field intensity of ~ 0.112 mV m^{-1}.

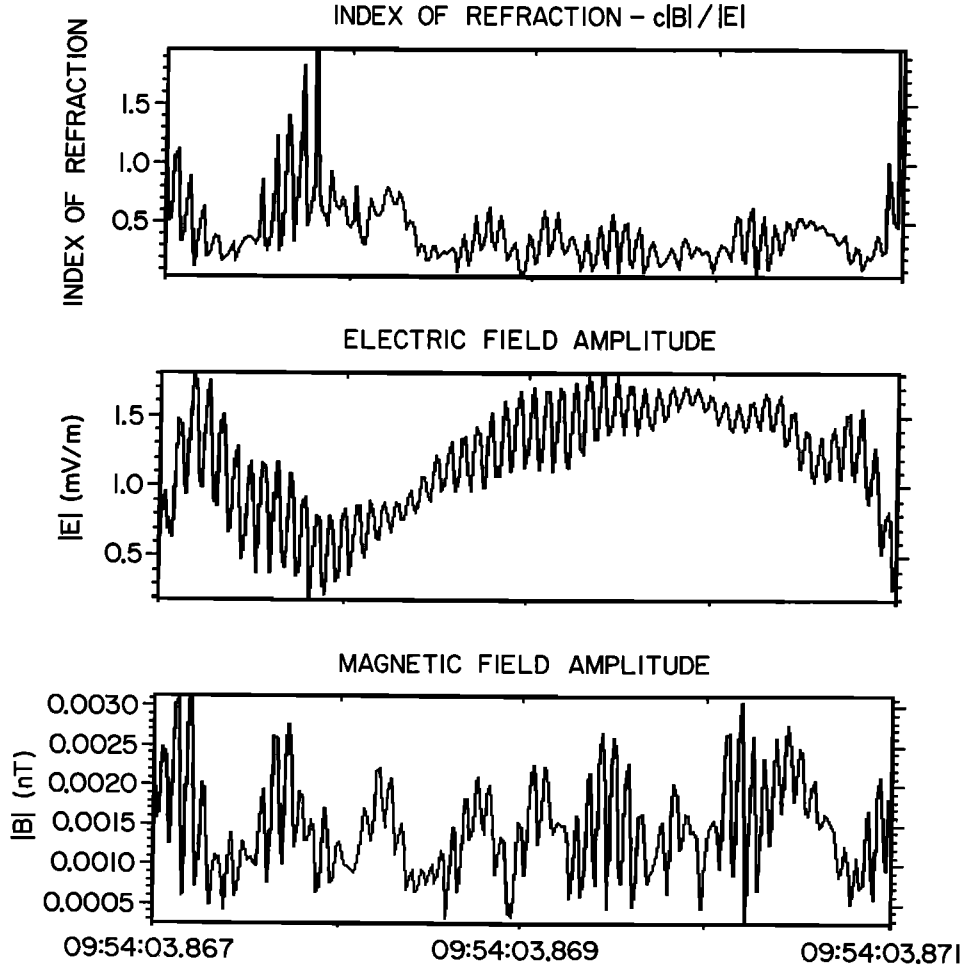

Figure 6. (top) Measured index of refraction, cB/E, for a 3.58-ms period during which intense wave activity near f_{UH} was observed. (middle, bottom) The calibrated electric and magnetic field waveforms, respectively.

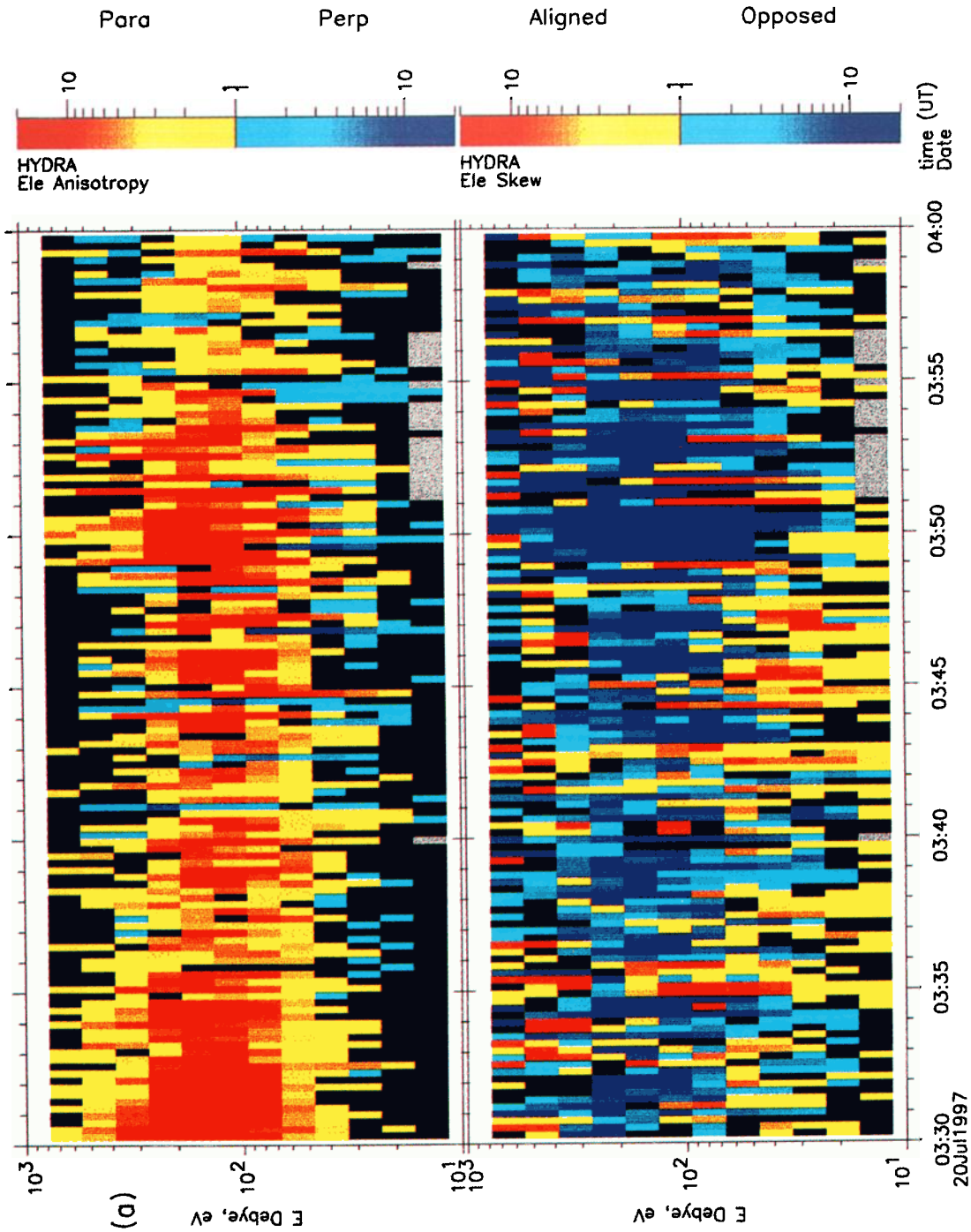

Plate 5. (a) Spectogram of the (top) electron anisotropy and (bottom) skew, from the HYDRA data for the time period 0330-0400 UT. The anisotropy measures if the particle distribution is parallel or perpendicular. The skew determines if the distribution is field-aligned or field-opposed to the magnetic field. During this time period the electron distribution for $E \geq 50$ eV is essentially parallel and moving opposed to the magnetic field (away from Earth). (b) Same as Plate 5a but for the later time period of 0640-0700 UT. Again, the top panel shows a distribution dominantly parallel to B. The bottom panel indicates electron beams moving away from the Earth with a particularly intense example near 0650 UT coincident with EEC wave intensification.

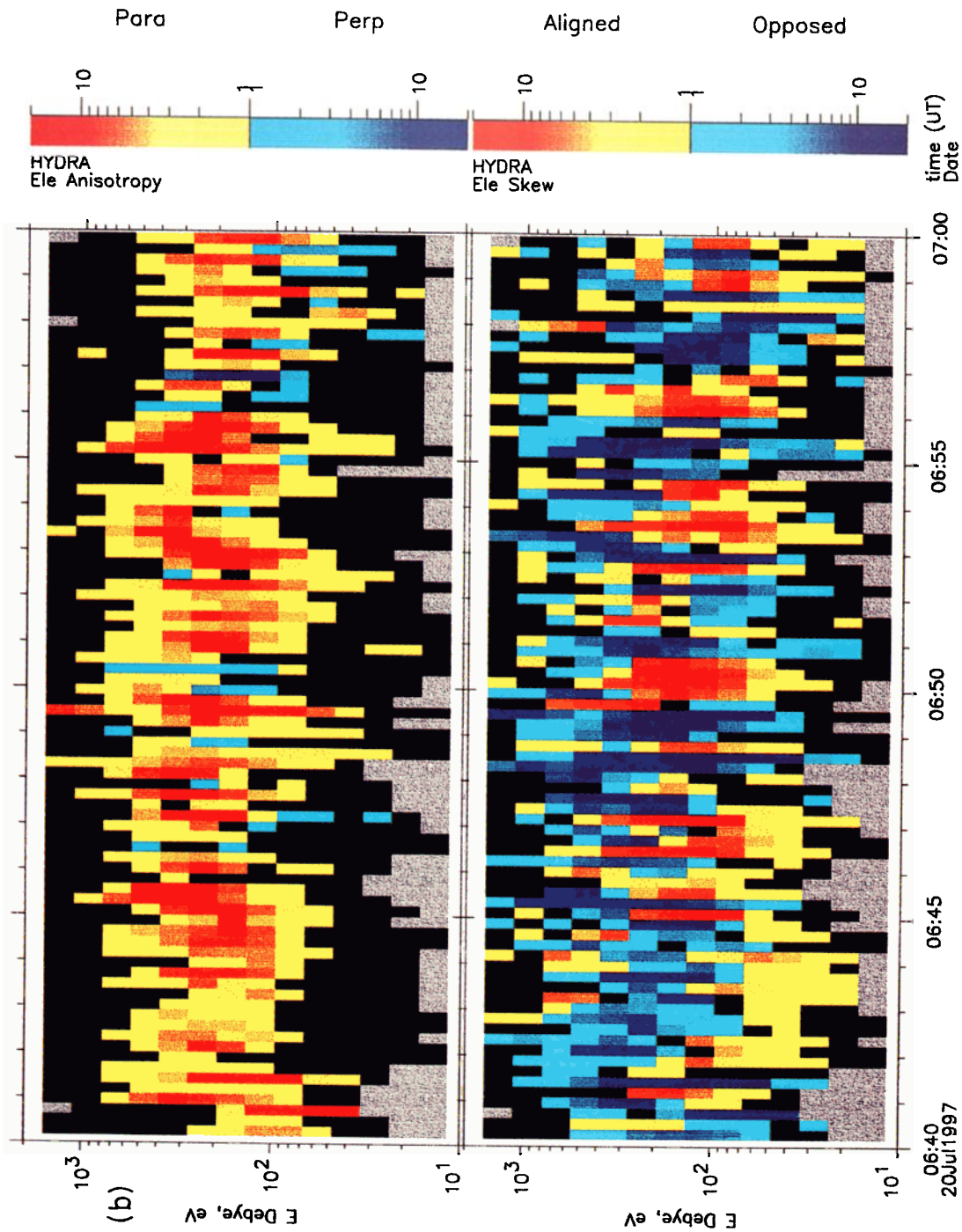

Plate 5. Continued.

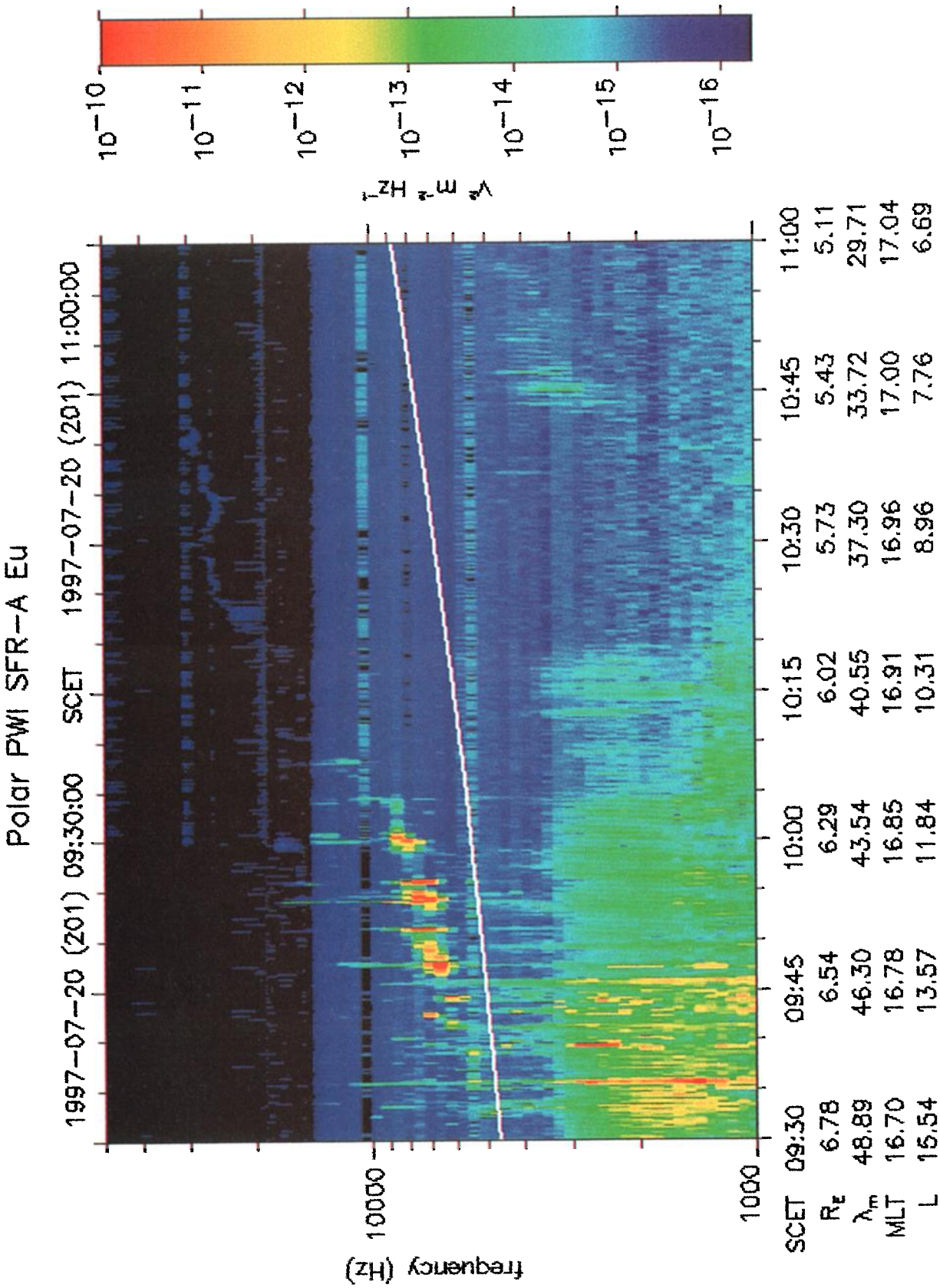

Plate 6. Spectrogram for a period nearer the plasmasphere with narrowband emissions believed to be due to the upper hybrid resonance mixed with electromagnetic oscillations.

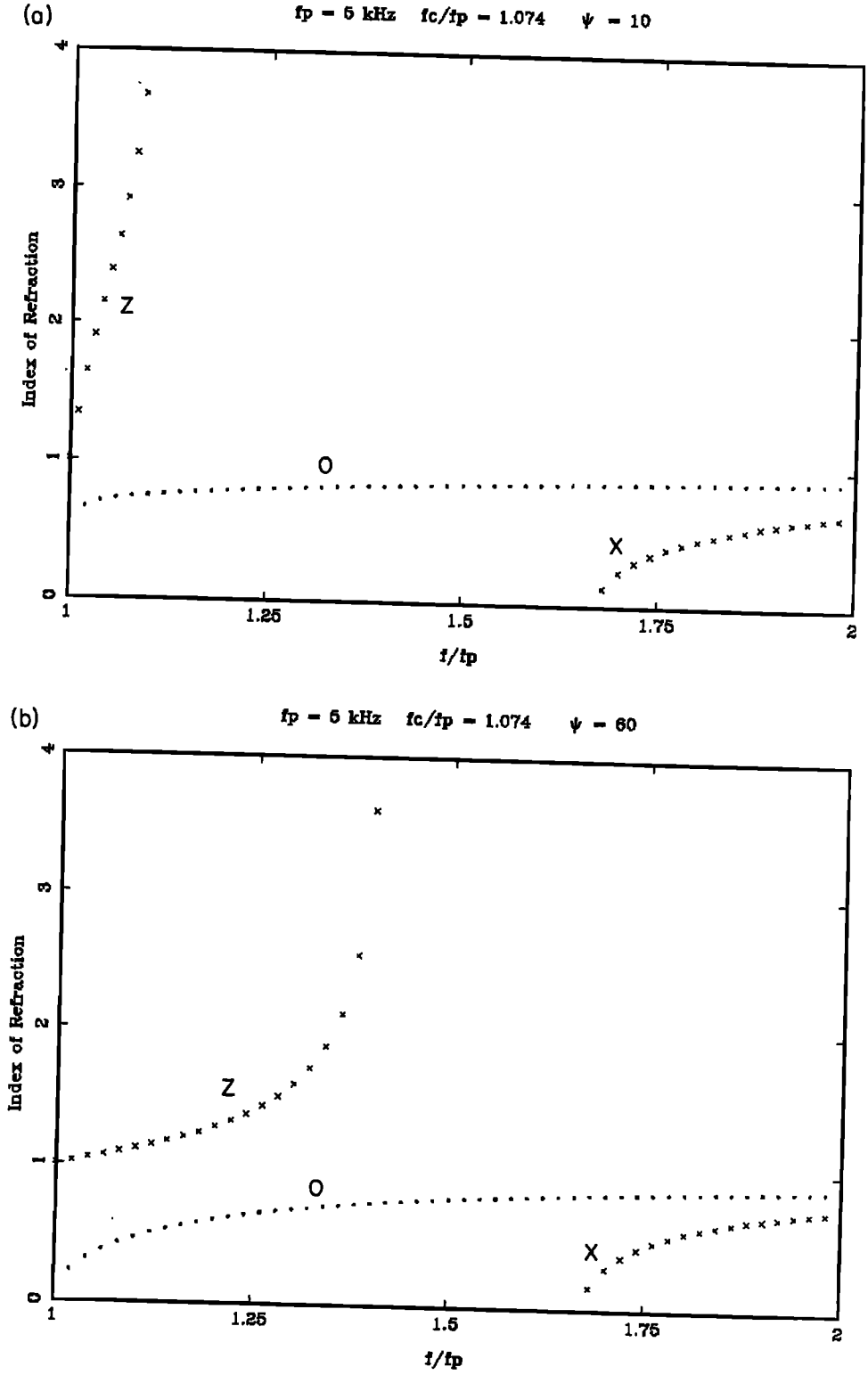

Figure 7. Theoretical cold plasma indices of refraction for a plasma with f_p = 5 kHz and f_c = 5.37 kHz (for 0954:03 UT) for wave normal angles of (a) 10° and (b) 60°. The wavemodes are indicated on the curves.

upper hybrid emissions mixed with some electromagnetic emissions. Polarization measurements of the electromagnetic (EM) emission show both left-handed and right-handed oscillations, propagating at wave normal angles ranging from 0° to 90°, but typically near ~ 60°. These measurements were made using a minimum variance procedure applied to the magnetic field data from the high-frequency waveform receiver. The Poynting vector is calculated from the electric and magnetic field results [cf. *Pickett et al.*, 1999].

The narrowband emissions shown for July 20, 1997, are typical of many other examples seen by PWI over the polar cap. These emissions are consistent with electrostatic electron cyclotron waves and harmonics. The plasma frequency is most likely larger than the cyclotron frequency for much of the polar pass, and the whistler

mode emission is attenuated near f_c. For this scenario ($f_p > f_c$ and $f_c < f < f_p$), electron cyclotron emission may be generated in the presence of beam and loss cone distributions. As seen in Figure 4 and Plate 6, electron beams at energies less than 1 keV are present during the observations of the EEC waves. These results are consistent with those of *Farrell et al.* [1990], who observed a correlation of similar waves seen in the cusp with beaming electrons with energies of a few hundred eV. Some weak magnetic field components associated with the narrowband upper hybrid emission observations are consistent with O mode and Z mode.

Acknowledgments. We thank J. Dowell for graphics software, J. Hospodarsky for text editing, and J. Chrisinger for drafting assistance. This work was supported under grants NAG5-7943 and NAG5-4497 with NASA/Goddard Space Flight Center.

Janet G. Luhmann thanks David Schriver and another referee for their assistance in evaluating this paper.

References

Bernstein, I. B., Waves in a plasma in a magnetic field, *Phys. Rev.*, *109*, 10, 1958.

Farrell, W. M., D. A. Gurnett, J. D. Menietti, H. K. Wong, C. S. Lin, and J. L. Burch, Wave intensifications near the electron cyclotron frequency within the polar cusp, *J. Geophys. Res.*, *95*, 6493, 1990.

Gurnett, D. A., S. D. Shawhan, and R. R. Shaw, Auroral hiss, Z mode radiation, and auroral kilometric radiation in the polar magnetosphere: DE 1 observations, *J. Geophys. Res.*, *88*, 329, 1983.

Gurnett, D. A., et al., The Polar plasma wave instrument, *Space Sci. Rev.*, *71*, 597, 1995.

Krall, N. A., and A. W. Trivelpiece, *Principles of Plasma Physics*, p. 410, McGraw-Hill, New York, 1973.

Kurth, W. S., M. Ashour-Abdalla, L. A. Frank, C. F. Kennel, D. A. Gurnett, D. D. Sentman, and B. G. Burek, A comparison of intense electrostatic waves near f_{UHR} with linear instability theory, *Geophys. Res. Lett.*, *6*, 487, 1979a.

Kurth, W. S., J. D. Craven, L. A. Frank, and D. A. Gurnett, Intense electrostatic waves near the upper hybrid resonance frequency, *J. Geophys. Res.*, *84*, 4145, 1979b.

Mosier, S. R., M. L. Kaiser, and L. W. Brown, Observations of noise bands associated with the upper hybrid resonance by the IMP 6 radio astronomy experiment, *J. Geophys. Res.*, *78*, 1673, 1973.

Pickett, J. S., J. D. Menietti, J. H. Dowell, D. A. Gurnett, and J. D. Scudder, Polar spacecraft observations of the turbulent outer cusp/magnetopause boundary layer of Earth, *Nonlinear Processes Geophys.*, *6*, 195, 1999.

Pickett, J. S., J. R. Franz, J. D. Scudder, J. D. Menietti, D. A. Gurnett, G. B. Hospodarsky, R. M. Braunger, P. M. Kintner, and W. S. Kurth, Plasma waves observed in the cusp turbulent boundary layer: An analysis of high time resolution wave and particle measurements from the Polar spacecraft, *J. Geophys. Res.*, this issue.

Scudder, J., et al., HYDRA-A 3-dimensional electron and ion hot plasma instrument for the Polar spacecraft of the GGS Mission, *Space Sci. Rev.*, *71*, 459, 1995.

Shaw, R. R., and D. A. Gurnett, Electrostatic noise bands associated with the electron gyrofrequency and plasma frequency in the outer magnetosphere, *J. Geophys. Res.*, *80*, 4259, 1975.

Tataronis, J. A., and F. W. Crawford, Cyclotron harmonic wave propagation and instabilities, I., Perpendicular propagation, *J. Plasma Phys.*, *4*, 231, 1970.

Winglee, R. A., J. D. Menietti, and H. K. Wong, Numerical simulations of bursty radio emissions from planetary magnetospheres, *J. Geophys. Res.*, *97*, 17,131, 1992.

Wong, H. K., and M. L. Goldstein, Electron cyclotron wave generation by relativistic electrons, *J. Geophys. Res.*, *99*, 235, 1994.

Young, T. S. T., J. D. Callen, and J. E. McCune, High-frequency electrostatic waves in the magnetosphere, *J. Geophys. Res.*, *78*, 1082, 1973.

D. A. Gurnett, J. D. Menietti, J. S. Pickett, and J. D. Scudder, Department of Physics and Astronomy, University of Iowa, Van Allen Hall, Iowa City, IA 52242-1479. (donald-gurnett@uiowa-edu; pickett@uiowa.edu; jack-scudder@uiowa.edu; jdm@space.physics.uiowa.edu)

(Received May 1, 2000; revised August 3, 2000;
accepted August 24, 2000.)